Polyoxometalate, Cationic Cluster and γ-Cyclodextrin. From Primary Interactions to Supramolecular Hybrid Materials

Mhamad Aly Moussawi, † Nathalie Leclerc-Laronze,† Sébastien Floquet,† Pavel A. Abramov,ǂ, £Maxim, N. Sokolov, ǂ, £ Stéphane Cordier,§ Anne Ponchel,‡ Eric Monflier,‡ Hervé Bricout,‡David Landy,∫ Mohamed Haouas,† Jérôme Marrot, † and Emmanuel Cadot†

† Institut Lavoisier de Versailles UMR 8180, UVSQ, Université Paris-Saclay, 78035 Versailles, France.

§ Institut des Sciences Chimiques de Rennes UMR 6226, Université de Rennes 1,

‡ Univ. Artois, CNRS, Centrale Lille, ENSCL, Univ. Lille, UMR 8181, Unité de Catalyse et Chimie du Solide, 62300 Lens, France

∫ Unité de Chimie Environnementale et Interactions sur le Vivant EA 4492, SFR Condorcet FR CNRS 3417, Université du Littoral Côte d'Opale, 59140 Dunkerque, France.

ǂ Nikolaev Institute of Inorganic Chemistry SB RAS, Novosibirsk, Russia.

£ Novosibirsk State University, Novosibirsk, 630090, Russia.

Supporting information

Table of Content:

1. General methods

Fourier Transformed Infrared (FT-IR) spectra were recorded on a 6700 FT-IR Nicolet spectrophotometer, using diamond ATR technique. The spectra were recorded on non-diluted compounds and ATR correction was applied.

UV-vis spectra were recorded on a Perkin-Elmer Lambda-750 using calibrated 0.1 cm Quartz-cell.

Elemental analyses (C, H, N, S) were carried out by the analytical service of the CNRS at Gif sur Yvette, France. **Quantitative analyses** of metals were carried out by ICP analysis and Fluo-X analysis and were performed in UCCS laboratory in Lille, France. These elemental analyses were performed by inductively coupled plasma-optic emission spectroscopy 720-ES ICP-OES (Agilent) with axially viewing and simultaneous CCD detection.

Energy-dispersive X-ray spectroscopy. EDX measurements were performed using a SEM-FEG (Scanning Electron Microscope enhanced by a Field Emission Gun) equipment (JSM 7001-F, Jeol). The measures were acquired with a SDD XMax 50 mm^2 detector and the Aztec (Oxford) system working at 15 kV and 10 mm working distance. The quantification is realized with the standard library provided by the constructor using Lα lines.

Water and cyclodextrin contents were determined by thermal gravimetric (TGA) analysis with a Mettler Toledo TGA/DSC 1, STAR^e System apparatus under oxygen flow (50 mL min^{-1}) at a heating rate of 5°C min^{-1} up to 700°C.

NMR studies. All solution NMR spectra were measured in D_2O at 25 °C when it is not specified. ^1H and ^{31}P NMR spectra were obtained on a Bruker Avance 400 spectrometer at Larmor frequencies 400.1 and 162.0 MHz respectively, using 5 mm standard NMR tubes. The 1D ^1H spectra were recorded with one pulse sequence at 30° flip angle (pulse duration 2.4 μs), using 1 s recycle delay, 1.6 s acquisition time, and 16 number of scans. Variable temperature ^1H NMR experiments were performed in the temperature range 20-80 °C after at least 30 min of sample temperature stabilization delay. The ^{31}P NMR spectra were run with 7.7 μs pulse duration (45° flip angle), 15 s recycle delay, 1 s acquisition time, and an accumulation of 32 transients. 2D ^1H-^1H COSY and EXSY spectra were carried out on some selected samples using standard phase sensitive pulse sequences in States mode and 1 s mixing time in EXSY experiment. Translational diffusion measurements were performed using Bruker's "ledbpgs2s" stimulated echo DOSY pulse sequence including bipolar and spoil gradients. Apparent diffusion coefficients were obtained using an adapted algorithm based on the inverse Laplace transform stabilized by maximum entropy (M.A. Delsuc, T.E. Malliavin, Anal. Chem. 1998, 70, 2146–2148). The ^{183}W NMR spectra were measured on a Bruker Avance 500 spectrometer at a resonance frequency of

20.8 MHz equipped with a specific low-gamma nuclei 10 mm probehead. Chemical shifts are reported relative to TMS (^{1}H), 85% H_3PO_4 (^{31}P), and 1 M aq. Na_2WO_4 (^{183}W), using secondary references in case of ^{183}W (D_2O/H_2O solution of $H_4SiW_{12}O_{40}$ observed at -103.8 ppm).

Electrospray Ionization Mass Spectrometry. Electrospray ionization (ESI) mass spectra were collected using a Q-TOF instrument supplied by WATERS. Samples were solubilized in water at a concentration of 10^{-4} M and were introduced into the MS via an ACQUITY UPLC WATERS system whilst a Leucine Enkephalin solution was co-injected via a micro pump as internal standard.

Isothermal Titration Calorimetry (ITC). Formation constants and inclusion enthalpies were simultaneously determined for each γ-CD/$[P_2W_{18}O_{62}]^{6-}$, γ-CD/$[Ta_6Br_{12}(H_2O)_6]^{2+}$ and γ-CD/$[P_2W_{18}O_{62}]^{6-}$/$[Ta_6Br_{12}(H_2O)_6]^{2+}$ systems by the use of an isothermal calorimeter (ITC_{200}, MicroCal Inc., USA). See paragraph §5 for further details.

Electrochemistry. Purified water was used throughout. It was obtained by passing water through a RiOs 8 unit followed by a Millipore-Q Academic purification set. All reagents were of high-purity grade and were used as purchased without further purification. Cyclic voltammetric (CV) experiments were carried out with an Methrohm Autolab PGSTAT12 potentiostat/galvanostat associated with a GPES electrochemical analysis system (EcoChemie). Measurements were performed at room temperature in a conventional single compartment cell. A glassy carbon (GC) electrode with a diameter of 3 mm was used as the working electrode. The auxiliary electrode was a Pt plate placed within a fritted-glass isolation chamber and potentials are quoted against a saturated calomel electrode (SCE). The solutions were deaerated thoroughly for at least 30 minutes with pure argon and kept under a positive pressure of this gas during the experiments.

Single-Crystal X-ray diffraction analysis. Intensity data collections were carried out at T = 200(2) K with a Bruker D8 VENTURE diffractometer equipped with a PHOTON 100 CMOS bidimensional detector using a high brilliance IμS microfocus X-ray Mo Ka monochromatized radiation (λ = 0.71073 Å) or at 100(2) K using X-Ray synchrotron beam line (λ = 0.72925 Å) at PROXIMA2 source in SOLEIL Laboratory (see Table S1). Crystals were glued in paratone oil to prevent any loss of crystallization water. An empirical absorption correction was applied using the SADABS program[1] based on the method of Blessing.[2] The structures were solved by direct methods and refined by full-matrix least squares using the SHELX-TL package.[3] Heavier atoms (W or Ta) for each structure were initially located by direct methods. The remaining non-hydrogen atoms were located from Fourier differences and were refined with anisotropic thermal parameters. Positions of the hydrogen atoms belonging to the γ-cyclodextrins were calculated

and refined isotropically using the gliding mode. Further details about of the crystal structure determinations may be obtained free of charge via the Internet at http://pubs.acs.org. Crystallographic data for single-crystal X-ray diffraction studies are summarized in Table S1.

(1) G. M. Sheldrick, SADABS, program for scaling and correction of area detector data, University of Göttingen, Germany, **1997**.
(2) R.Blessing, *Acta Cryst*. **1995**, *A51*, 33.
(3) G. M. Sheldrick, *Acta Cryst*. **1990**, *A46*, 467 ; Sheldrick, G. M. SHELX-TL version 5.03, Software Package for the Crystal Structure Determination, Siemens Analytical X-ray Instrument Division : Madison, WI USA, **1994.**

Powder X-ray diffraction analysis. Powder X-ray diffraction data was obtained on a Brüker D5000 diffractometer using Cu radiation (λ = 1.54059 Å).

2. Syntheses

All reagents were purchased from commercial sources and used without further purification. **$K_6[P_2W_{18}O_{62}]•19H_2O$** was prepared according to the procedure published by Mbomekalle at al. (Mbomekalle, I. M.; Lu, Y. W.; Keita, B.; Nadjo, L. *Inorg. Chem. Commun.* **2004**, *7*, 86). Cesium and rubidium salts of $[P_2W_{18}O_{62}]^{6-}$ were prepared by addition of an excess of CsCl or of RbCl to an aqueous solution of $K_6[P_2W_{18}O_{62}]•19H_2O$. Their compositions were checked by FT-IR, TGA and EDX.

$KNa_5\{[P_2W_{18}O_{62}](C_{48}H_{80}O_{40})\}•3.5NaCl•23H_2O$ (POM@CD). A mixture of $K_6[P_2W_{18}O_{62}]•19H_2O$ (1.2 g; 0.24 mmol) and γ-cyclodextrin (γ-CD, 0.34 g; 0.24 mmol) in aqueous solution of NaCl (0.5 mol.L^{-1}; 25 mL) was stirred at 35°C for 15 min resulting in a clear solution. The clear solution was then stirred at room temperature for 15 min and was allowed to stand for crystallization in air. Needle-like colorless crystals of **POM@CD** suitable for single crystal X-ray diffraction appeared within 5 days. They were isolated by filtration and washed with cold water. Yield 1.22 g, 78 %. FT-IR spectrum is given in Figure S1. Elemental analysis for $C_{48}H_{126}Cl_{3.50}KNa_{8.5}O_{120}P_2W_{18}$ (FW = 6352,1 g.mol^{-1}) Calc. (found): H 1.98 (2.08); C 9.03 (9.25); Na 3.06 (2.95); K 0,61 (0.66); P 0.97 (1.00); W 52.1 (51.92). TGA showed a weight loss of 6.5% in the 20-220°C temperature range corresponding to the hydration water (calculated 6.7%) and a weight loss of 22.5 % in the 220-700°C range assigned to the loss of 1 CD and the 3.5 Cl (calculated 21.5 %).

$CsNa_5\{[P_2W_{18}O_{62}](C_{48}H_{80}O_{40})_2\}•1.2NaCl•23H_2O$ (POM@2CD). A solution of $Cs_6[P_2W_{18}O_{62}]•19H_2O$ (0.55 g; 0.1 mmol) in aqueous solution of NaCl (0.5 mol.L^{-1}; 18 mL) was

stirred at 30°C until the total dissolution of the solid. γ-CD (0.26 g; 0.2 mmol) was added to the resulting limpid solution that was stirred at room temperature for 20 min. The obtained mixture was allowed to stand for crystallization in air where needle-like colorless crystals of **POM@2CD** suitable for single crystal X-ray diffraction appeared within 8 days. They were isolated by filtration and washed with cold water. Yield 0.42 g, 55 %. FT-IR spectrum is given in Figure S1. Elemental analysis for $C_{96}H_{206}Cl_{1.2}CsNa_{6.2}O_{165}P_2W_{18}$ (FW = 7689.8 g/mol) Calc. (found): C 14.99 (14.43); Cs 1.73 (1.82); H 2.70 (2.78); Na 1.85 (2.08); P 0.81 (0.94); W 43.03 (44.45). TGA showed a weight loss of 5.63% in the 20-220°C temperature range corresponding to the hydration water (calculated 5.38%) and a weight loss of 32.7 % in the 220-700°C range assigned to the loss of 2 CD (calculated 33.7 %).

$Rb_4K_{1.5}Na_{0.5}\{[P_2W_{18}O_{62}](C_{48}H_{80}O_{40})_3\}\bullet 35H_2O$ (POM@3CD). A solution of $Rb_6[P_2W_{18}O_{62}]\bullet 19H_2O$ (1.5 g; 0.29 mmol) in 25 mL distilled water was stirred at 30°C until the total dissolution of the solid. γ-CD (1.125 g; 0.86 mmol) were added to the resulting limpid solution that was stirred at room temperature for 20 min. The obtained mixture was allowed to stand for crystallization in air where hexagonal colorless crystals of **POM@3CD** suitable for single crystal X-ray diffraction appeared within 7 days. They were isolated by filtration and washed with ethanol and ether. Yield 1.32 g md, 48 %. FT-IR spectrum is given in Figure S1. Elemental analysis for $C_{144}H_{310}K_{1.5}Na_{0.5}O_{217}P_2Rb_4W_{18}$ (FW = 9293,3 $g.mol^{-1}$) Calc. (found): C 18.6 (17.97); H 3.33 (3.19); K 0.63 (0.57); Na 0.12 (0.01); P 0.66 (0.85); Rb 3.67 (3.60); W 35.60 (34.83). TGA showed a weight loss of 7.12% in the 20-220°C temperature range corresponding to the hydration water (calculated 7.66%) and a weight loss of 40.34 % in the 220-700°C range assigned to the loss of 3 CD (calculated 41.45 %).

$\{[Ta_6Br_{12}(H_2O)_6](C_{48}H_{80}O_{40})_2\}Br_2\bullet 14H_2O$, ($\{Ta_6\}$@2CD). (250 mg; 0.108 mmol) $[Ta_6Br_{12}(H_2O)_6]Br_2$ were dissolved in 10 mL distilled water resulting in a dark green solution. In a separate beaker, (312 mg; 0.22 mmol) γ-CD were dissolved in 5 mL of distilled water resulting in a clear limpid solution. The latter was added in one shot to the former, the obtained solution was stirred gently for 10 min and then allowed to stand for crystallization. Two days later, abundant quantity of square-like dark green crystals of **$\{Ta_6\}$@2CD** suitable for single crystal X-ray diffraction was obtained. Yield 405 mg, 73 %. FT-IR spectrum is given in Figure S2. Elemental analysis for $Br_{14}C_{96}H_{200}Ta_6$ (FW = 5156.2 g/mol) Calc. (found): C 22,34 (22.20) ; Br 21,69 (21,51) ; H 3.87 (3.9); Ta 21.05 (20.95). TGA showed a loss of 6.99% assigned to coordinated and hydration water molecules in the 20-120 °C temperature range (calculated 6.97%) and a loss of 66.9 % in the 120-500°C range corresponding to the loss of 2 CD and the 14 Br with the formation of Ta_2O_5 (calculated 67.3%).

Preparation of {Ta_6@2CD•POM}-based hydrogel Gel. $[Ta_6Br_{12}(H_2O)_6]Br_2$ (100 mg; 0.0432 mmol) were dissolved in 2 mL distilled water. Another solution of $K_6[P_2W_{18}O_{62}]$•$19H_2O$ (212 mg; 0.0432 mmol) and $C_{48}H_{80}O_{40}$•$6.6H_2O$ (121 mg; 0.0865 mmol) were dissolved in 5 mL distilled water. The former (green solution) was added dropwise to the latter (clear solution) while gently stirring. Each drop introduced into the solution coagulates and form a micelle-like green droplet. With the continuous addition of the tantalum solution, the viscosity of the solution increases gradually and the magnetic bar struggles to rotate. After the addition of the whole quantity of the green solution, the viscous mixture was stirred gently for five minutes. The resulting green mixture was allowed to stand for one hour in open air where a green gel is obtained. The gel maintains its viscosity and texture if left covered afterwards while it dries up if left in open air. Composition of the hydrogel was determined by elemental EDX after thoroughly washing the gel through successive centrifugation in excess water to removed mother liquor and then drying in air at room temperature. FT-IR spectrum of the gel after drying is given in Figure S2. Elemental analysis for $K_4[Ta_6Br_{12}(H_2O)_6][\gamma\text{-CD}]_2[P_2W_{18}O_{62}]$ ~60 H_2O : Calc.(found) Br 9.26 (10,04); C 11.13(11,93); H 2.82 (3,04); K 1.51 (1,43); P 0,59 (0,65); Ta 10.49 (11,82); W 31,99 (30,52).

Synthesis of Single crystals of $K_2H_2[Ta_6Br_{12}(H_2O)_6][\gamma\text{-CD}]_2[P_2W_{18}O_{62}].32.5H_2O$**.** Solutions similar to those used in the preparation of the gel were utilized in the crystallization process. Around 0.5 mL of each solution was introduced on opposite sides of a 0.5 cm diameter H-tube. Two drops of CF_3SO_3H 2 M were added to each side. Then distilled water was layered above both solutions until the H-tube was filled allowing slow diffusion on both sides. After one week needle-like green crystals are formed at the center of the tube. Crystals were isolated and characterized by XRD, FT-IR, TGA and EDX. Yield 50 mg, 47 %. FT-IR spectrum is given in Figure S2. TGA showed a weight loss of 6.50% assigned to coordinated and hydration water molecules in the 20-120 °C temperature range (calculated 6.00%) and a loss of 34.8 % in the 120-600°C range corresponding to the loss of the 2 CD and the 12 Br with the formation of K_2O, Ta_2O_5, P_2O_5 and WO_3 (calculated 34.2%).

Elemental analysis for $Br_{12}C_{96}H_{239}K_2O_{180.5}P_2Ta_6W_{18}$: calc.(found) Br 9.81(10,21) ; C 11.78(11,82) ; H 2.44(2.53) ; K 0.80(0,78) ; P 0.63(0,61) ; Ta 11.10(11,43) ; W 33.86(32,54). FW = 9772.8 g/mo

3. FT-IR Spectra

Fourier Transformed Infrared (FT-IR) spectra were recorded using diamond ATR technique. The spectra were recorded on non-diluted compounds and ATR correction was applied.

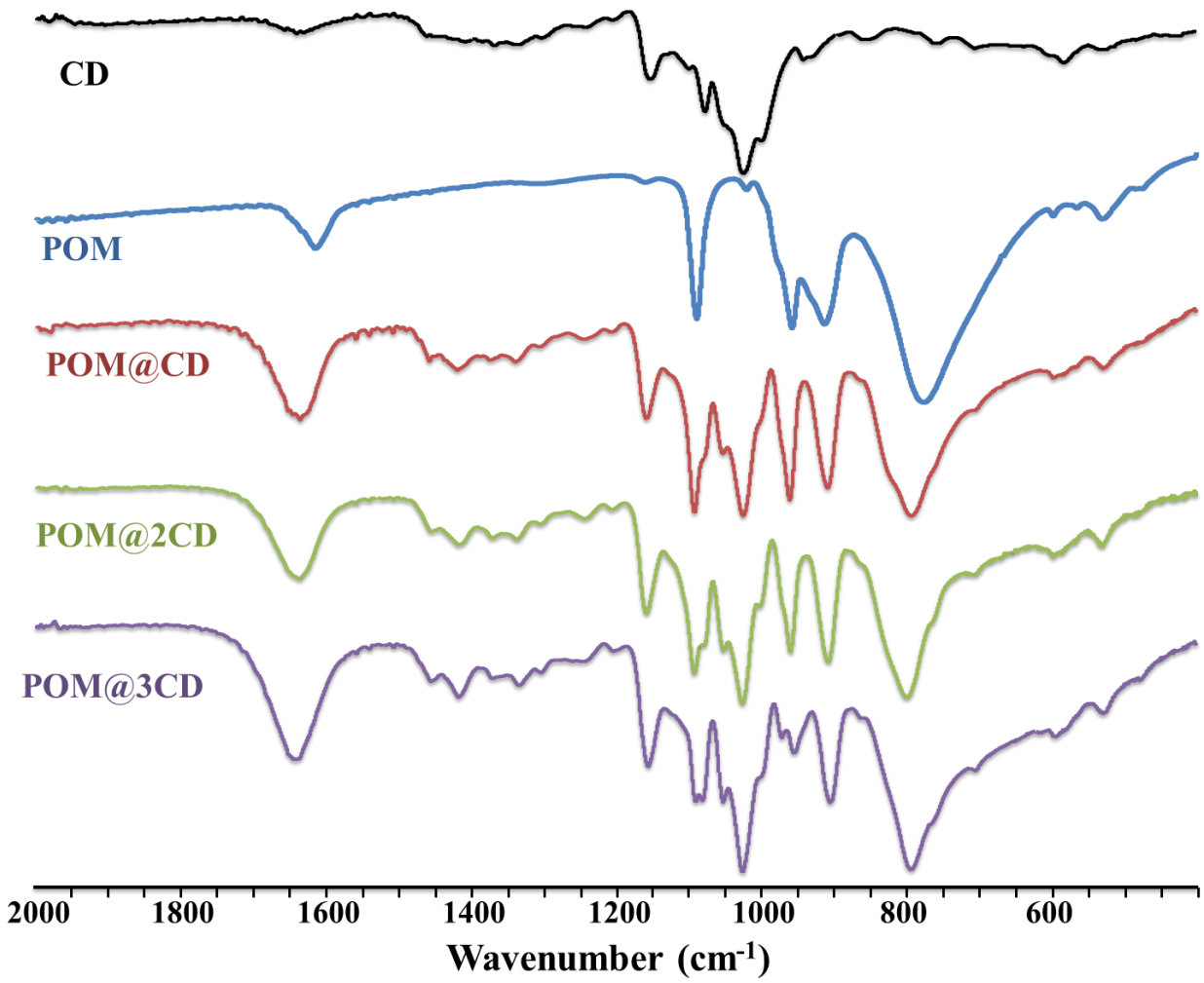

Figure S1. FT-IR spectra of compounds POM@CD, POM@2CD, and POM@3CD, in comparison with the FT-IR spectra of the precursor $K_6[P_2W_{18}O_{62}].19H_2O$ (POM) and of the γ-cyclodextrin (CD). From POM@CD to POM@3CD, the ratio of the bands of CD compared to that of the POM clearly increases (see in the 950-1150 cm^{-1} range).

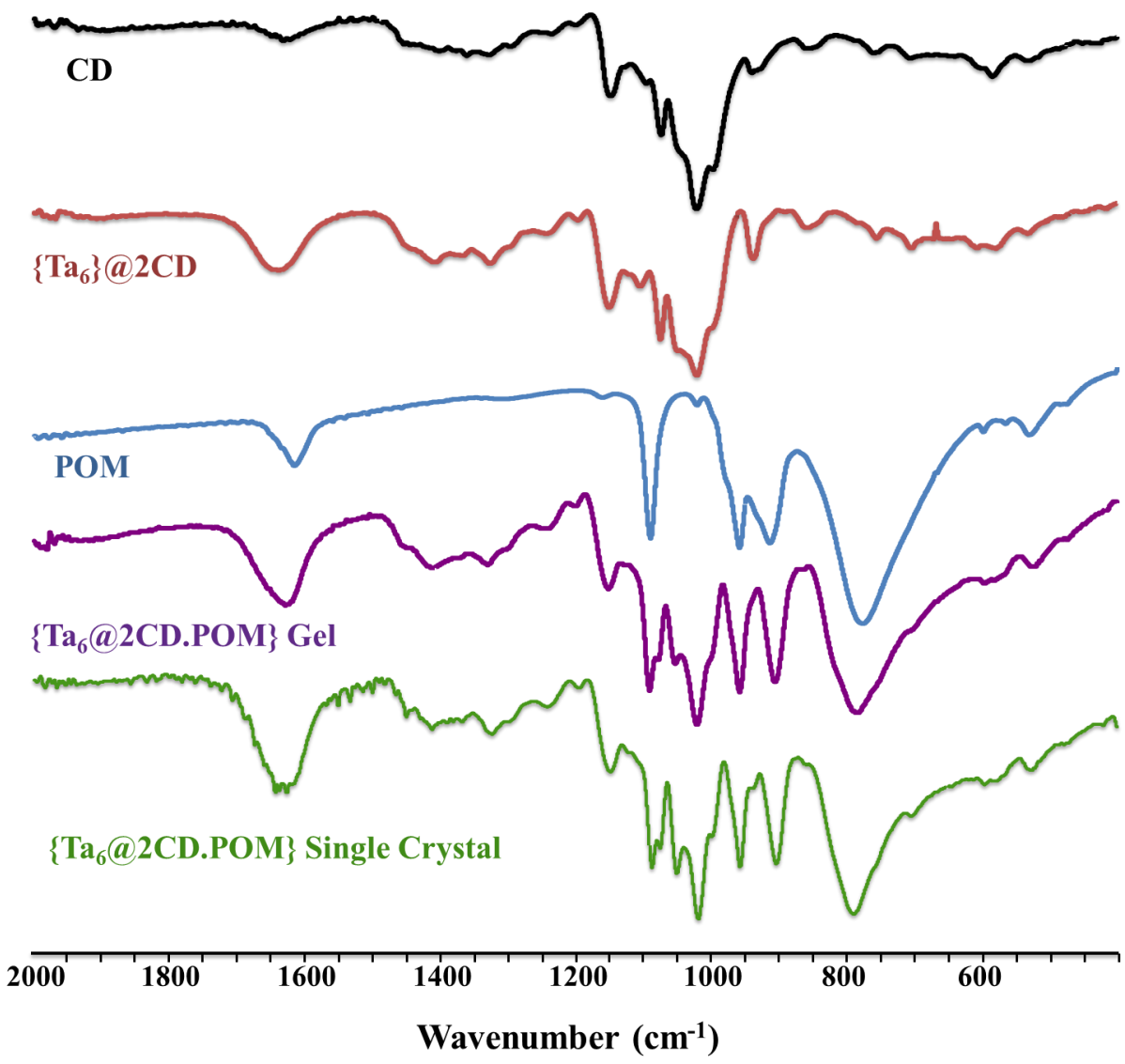

Figure S2. FT-IR spectra of compounds {Ta_6@2CD} and {Ta_6@2CD.POM}, as gel and single crystals, in comparison with the FT-IR spectra of the precursor $K_6[P_2W_{18}O_{62}].19H_2O$ (POM) and of the γ-cyclodextrin (CD). The FT-IR spectrum of the cluster $[Ta_6Br_{12}(H_2O)_6]^{2+}$ is silent. Therefore, the FT-IR spectrum of {Ta_6@2CD} almost corresponds to that of the CD alone. The FT-IR spectrum of the gel {Ta_6@2CD.POM} was performed after drying and corresponds well to that obtained with single crystals of {Ta_6@2CD.POM}.

4. Single crystal X-ray diffraction.

4.1. Material & Methods.

Intensity data collections were carried out at T = 200(2) K with a Bruker X8 APEX2 CCD, using the MoKα wavelength (λ = 0.71073 Å) or at 100(2) K using X-Ray synchrotron beam line (λ = 0.72925 Å) at PROXIMA2 source in SOLEIL Laboratory (see table S1). Crystals were glued in paratone to prevent any loss of crystallization water. An empirical absorption correction was applied using the SADABS program[1] based on the method of Blessing.[2] The structures were solved by direct methods and refined by full-matrix least squares using the SHELX-TL package.[3] Heavier atoms (W or Ta) for each structure were initially located by direct methods. The remaining non-hydrogen atoms were located from Fourier differences and were refined with anisotropic thermal parameters. Positions of the hydrogen atoms belonging to the coordinated acetate were calculated and refined isotropically using the gliding mode. Selected Crystallographic data for single-crystal X-ray diffraction studies are summarized in Table S1. CCDC 1561363, 1561364, 1561365, 1561366 and 1561367 also contain the supplementary crystallographic data for this paper. These data can be obtained free of charge via www.ccdc.cam.ac.uk/data_request/cif. Further details about of the crystal structure determinations may be obtained free of charge via the Internet at http://pubs.acs.org.

(1) G. M. Sheldrick, SADABS, program for scaling and correction of area detector data, University of Göttingen, Germany, **1997**.

(2) R.Blessing, *Acta Cryst*. **1995**, *A51*, 33.

(3) G. M. Sheldrick, *Acta Cryst*. **1990**, *A46*, 467 ; Sheldrick, G. M. SHELX-TL version 5.03, Software Package for the Crystal Structure Determination, Siemens Analytical X-ray Instrument Division : Madison, WI USA, **1994**

4.2. Selected crystallographic parameters of the single-crystal X-ray diffraction structural analysis.

Table S1.

Compound	POM@CD	POM@2CD	POM@3CD	Ta_6@2CD	Ta_6@2CD@POM
Formula	$C_{48}H_{116}Cl_{3.50}KNa_{8.50}O_{120}P_2W_{18}$	$C_{96}H_{206}Cl_{1.20}CsNa_{6.20}O_{165}P_2W_{18}$	$C_{144}H_{310}K_{1.50}Na_{0.50}O_{217}P_2Rb_4W_{18}$	$C_{96}H_{200}Br_{14}O_{100}Ta_6$	$C_{96}H_{239}Br_{12}K_2O_{180.50}P_2Ta_6W_{18}$
FW, g.mol^{-1}	6343.23	7689.82	9297.17	5158.99	9775.92
T, K	100	200	200	200	100
crystal size (mm)	0.08 × 0.06 × 0.04	0.30 × 0.04 × 0.02	0.30 × 0.28 × 0.03	0.20 × 0.12 × 0.06	0.01 × 0.01 × 0.01
crystal system	Orthorhombic,	Orthorhombic	Trigonal	Tetragonal	Tetragonal
space group	$P2_12_12_1$	$P2_12_12_1$	$P321$	$I422$	$P4_12_12$
a, Å	17.671 (4)	17.2589 (16)	21.1963 (4)	23.8984 (11)	23.985 (3)
b, Å	24.533 (5)	31.374 (3)	21.1963 (4)	23.8984 (11)	23.985 (3)
c, Å	40.756 (8)	41.297 (3)	35.5050 (17)	34.8186 (19)	89.175 (18)
V, Å^3	17669 (6)	22362 (3)	13814.7 (8)	19886 (2)	51301 (18)
Z	4	4	2	4	8
ρ_{calc}, g.cm^{-3}	2.385	2.284	2.235	1.723	2.531
μ(Mo Kα), cm^{-1}	1.224	0.953	0.832	0.619	1.303
λ(Mo Kα), Å	0.72925	0.71073 Å	0.71073 Å	0.71073	0.72931
θ range, deg	θ_{max} = 25.5°, θ_{min} = 1.0°	θ_{max} = 25.1°, θ_{min} = 2.2°	θ_{max} = 30.0°, θ_{min} = 2.2°	θ_{max} = 25.1°, θ_{min} = 2.1°	θ_{max} = 25.6°, θ_{min} = 0.9°
data collected	184384	249509	168660	129482	532679
unique data	29038	38493	26908	8872	44271
unique data I>2σ(I)	21536	32586	20542	7074	22525
no. Parameters	855	2330	1142	521	1718
restraints	452	2915	3	10	878
$R_w(F^2)$	0.293	0.318	0.146	0.212	0.280
R(F)	0.097	0.130	0,049	0.072	0.103
GOF	1.03	1.11	1.02	1.14	1.01

4.3. Structural views of POM@nCD arrangements

4.3.1. POM@1CD

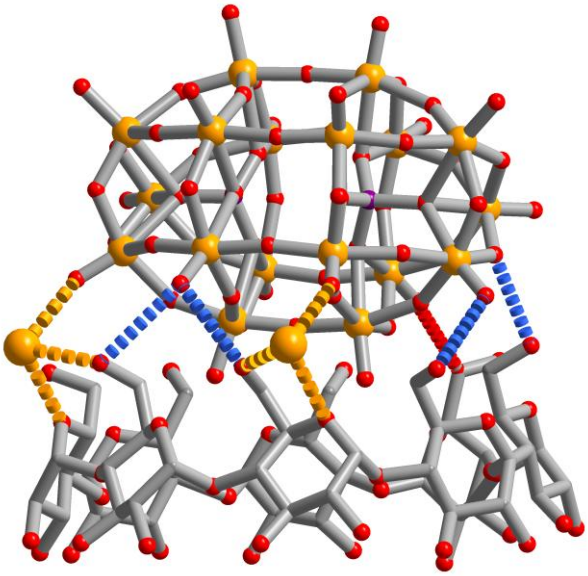

Figure S3. Structural representation of the POM@1CD arrangement showing the involvement of the potassium cations (yellow spheres) within the POM•••γ-CD interactions in addition to the hydrogen bonds (dotted blue sticks) and C-H•••O (red dotted stick).

4.3.2. POM@2CD

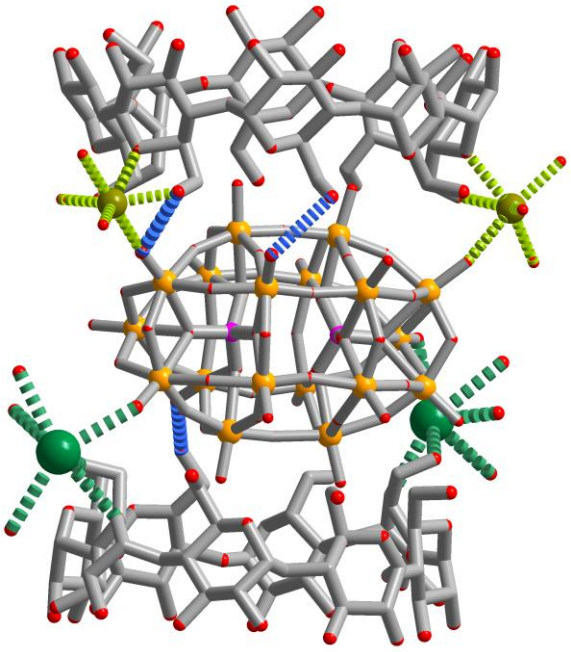

Figure S4. Structural representation of the POM@2CD arrangement showing the involvement of the cesium (dark-green spheres) and sodium cations (light-green spheres) within the POM•••γ-CD interactions in addition to the hydrogen bonds (dotted blue sticks).

4.3.3. POM@3CD

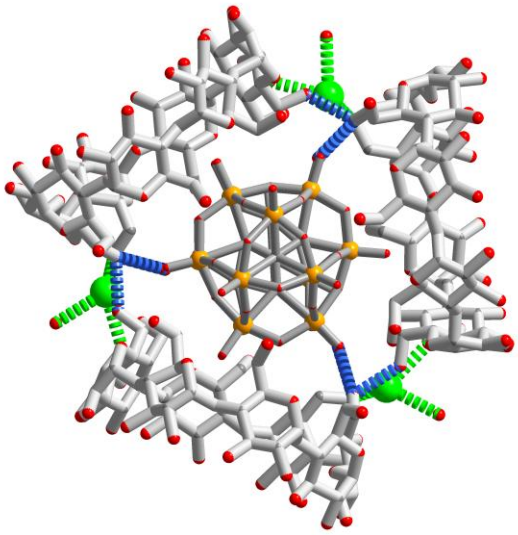

Figure S5. Structural representation of the POM@3CD arrangement along the C_3 axis showing the involvement of the rubidium cations (light-green spheres) within the POM•••γ-CD interactions in addition to the hydrogen bonds (dotted blue sticks).

4.3.4. Structural views of $\{Ta_6\}$@2CD arrangement

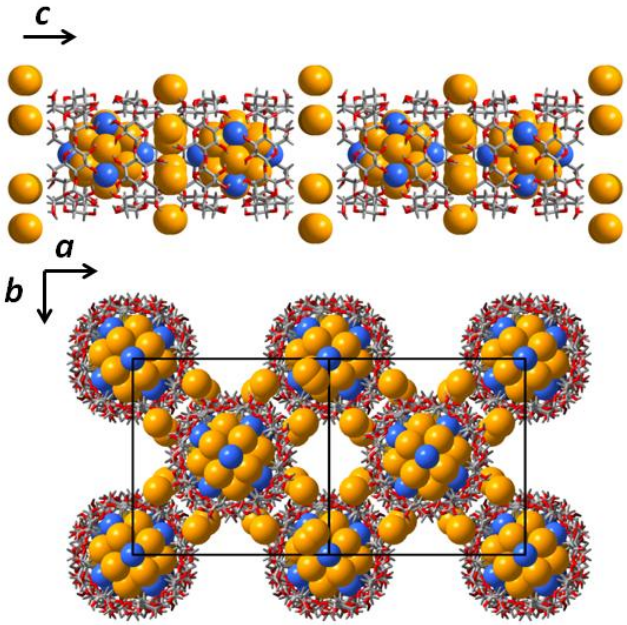

Figure S6. Representation of the $\{Ta_6\}$@2CD structure showing the tubular bamboo-like chains running along the c axis. The supramolecular host-guest assembly are alternately stacked through short (O•••O = 2.83Å) and long (O•••O = 6.78Å) intermolecular interaction involving the primary face of the γ-CD. These "bamboo-like" chains are mutually connected through the bromide counter ions to give the tetragonal cells. Color code : yellow sphere = Br; blue sphere = aqua ligand of the $\{Ta_6\}^{2+}$ cluster; the cyclodextrin are represented by grey sticks.

5. NMR data.

5.1. ^{31}P NMR

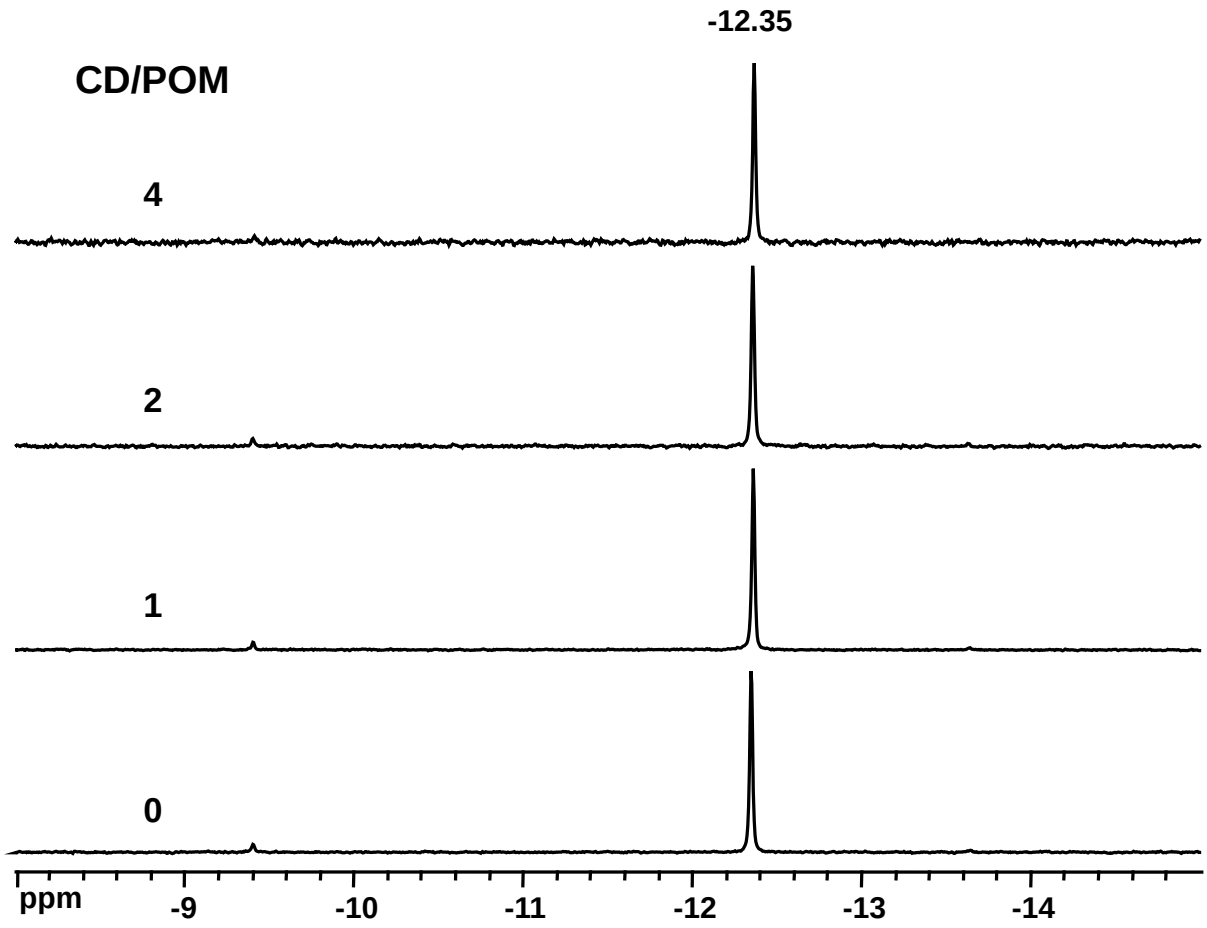

Figure S7. ^{31}P NMR spectra of $K_6[P_2W_{18}O_{62}]$ solution containing variable amounts of γ-CD showing little effect on the POM signal.

5.2. ^{183}W NMR

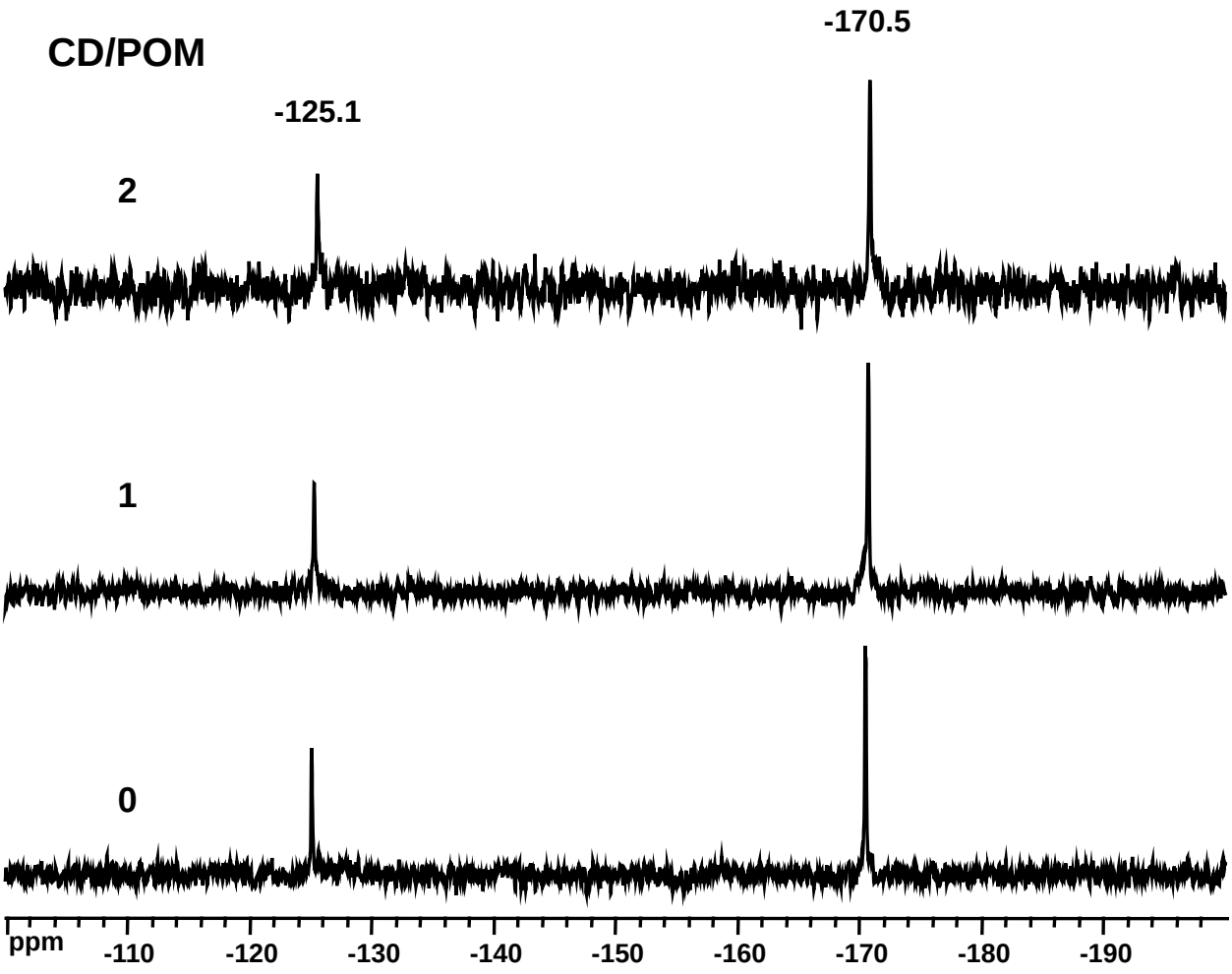

Figure S8. ^{183}W NMR spectra of $K_6[P_2W_{18}O_{62}]$ solution containing variable amounts of γ-CD showing little effect on the POM signals.

5.3. ^{1}H NMR titration

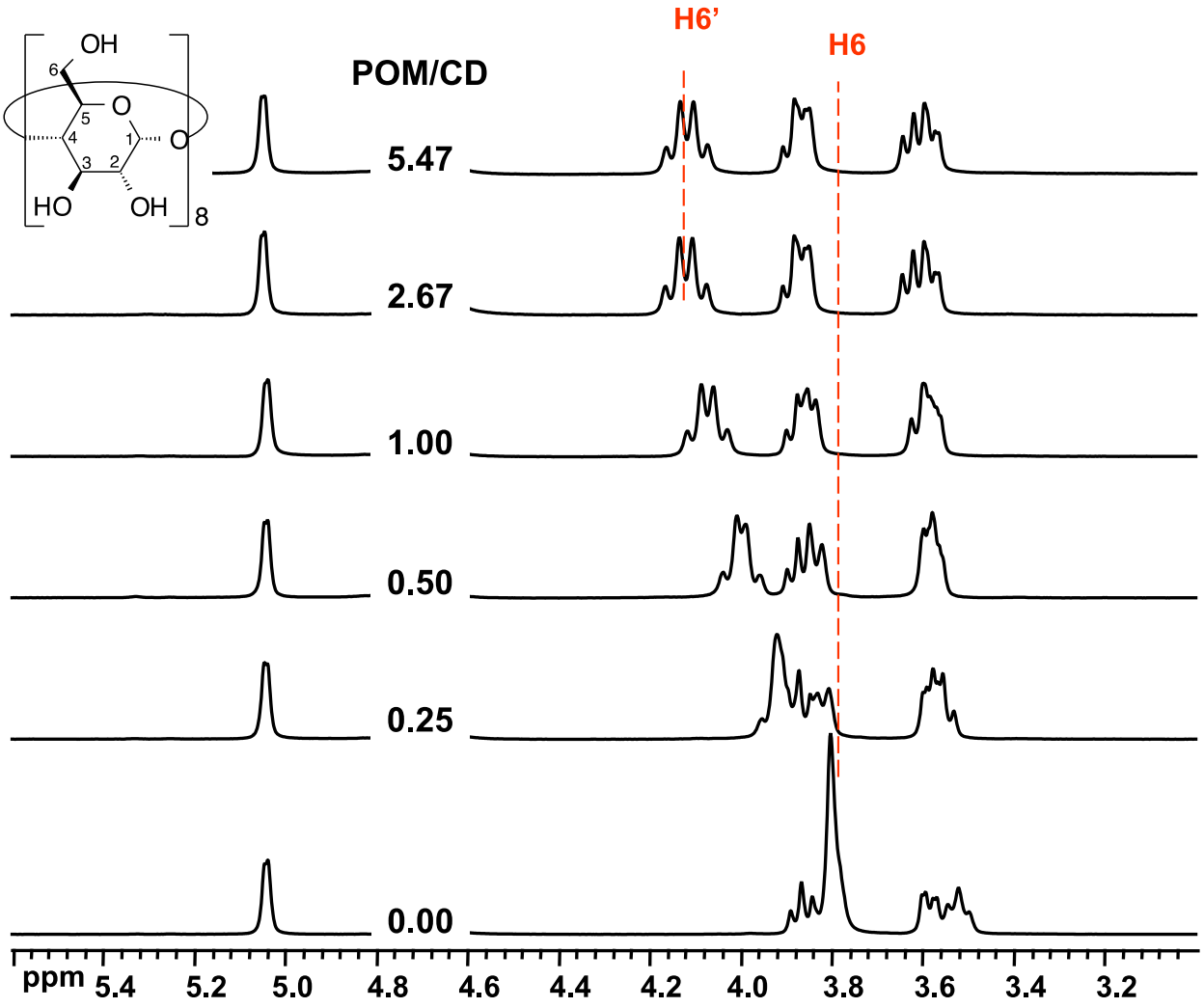

Figure S9. ^{1}H NMR spectra of γ-CD solution (3 mM) containing variable amounts of $K_6[P_2W_{18}O_{62}]$, showing effect on signal H_6 as a result of inclusion complex formation.

5.4. ^{31}P DOSY NMR

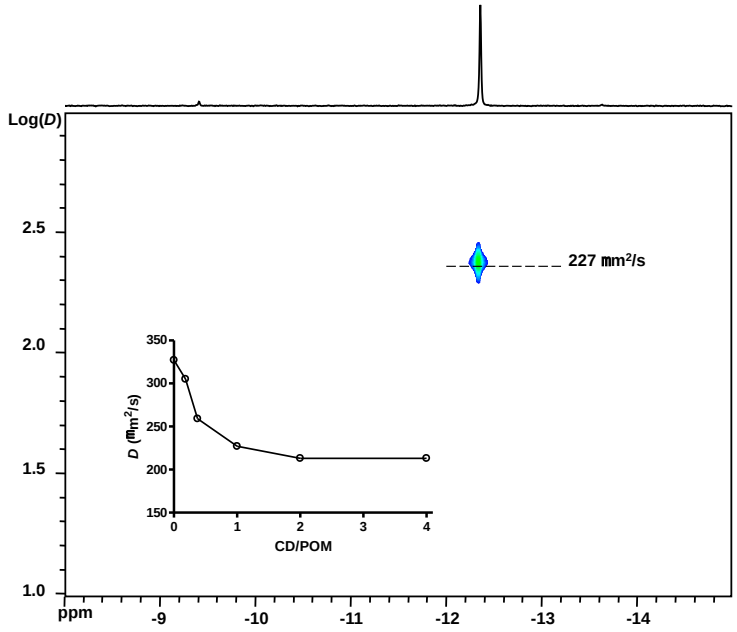

Figure S10. ^{31}P DOSY NMR spectrum of $K_6[P_2W_{18}O_{62}]$ solution (3 mM) containing equimolar amount of γ-CD. Inset: Evolution of diffusion coefficients measured as a function of CD/$[P_2W_{18}O_{62}]^{6-}$ molar ratio.

5.5. ^{1}H NMR DOSY

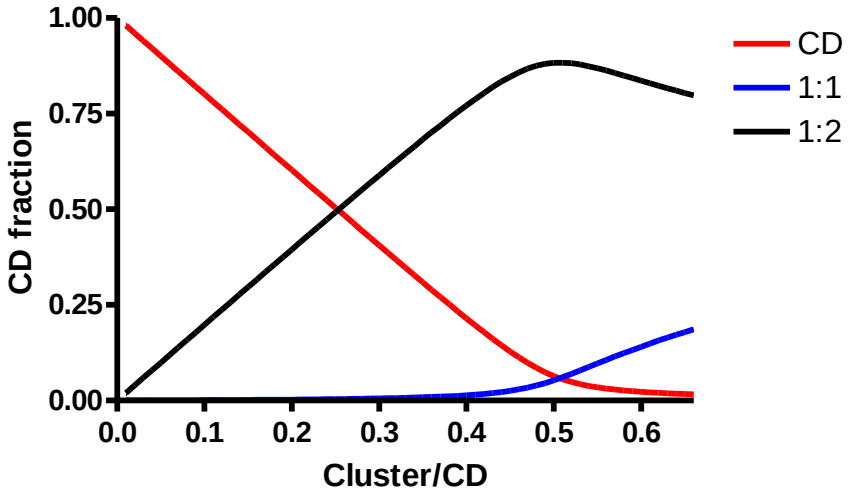

Figure S11. CD species distribution in NMR study conditions of Figure 5 (fixed [CD] = 1 mM) calculated with ITC binding constants for 1:1 and 1:2 inclusion complexes K_{11} = 1.5 10^5 M^{-1} and K_{12} = 1.3 10^5 M^{-1} (Table 1), showing the predominance of 1:2 complex with respect to 1:1 complex.

5.6. EXSY ^{1}H NMR

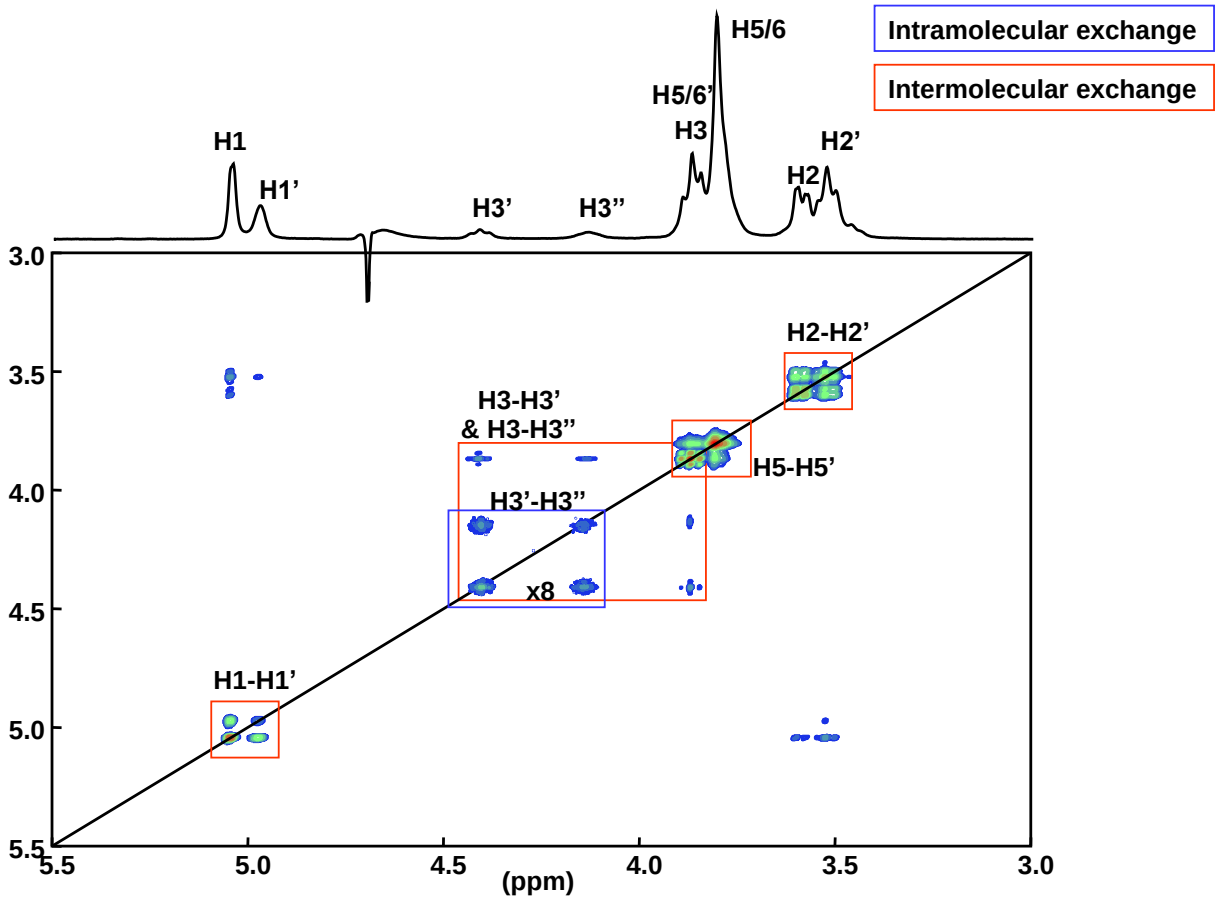

Figure S12. ^{1}H EXSY NMR spectrum of γ-CD solution (3 mM) containing $[Ta_6Br_{12}(H_2O)_6]Br_2$ in the molar ratio $[Ta_6Br_{12}(H_2O)_6]^{2+}$/CD = 0.25, showing exchange correlations between protons of free (H_n) and complexed (H_n') CDs, and protons of the two types of glucopyranose units (H_n' & H_n") present in the complexed CD.

5.7. VT ^{1}H NMR

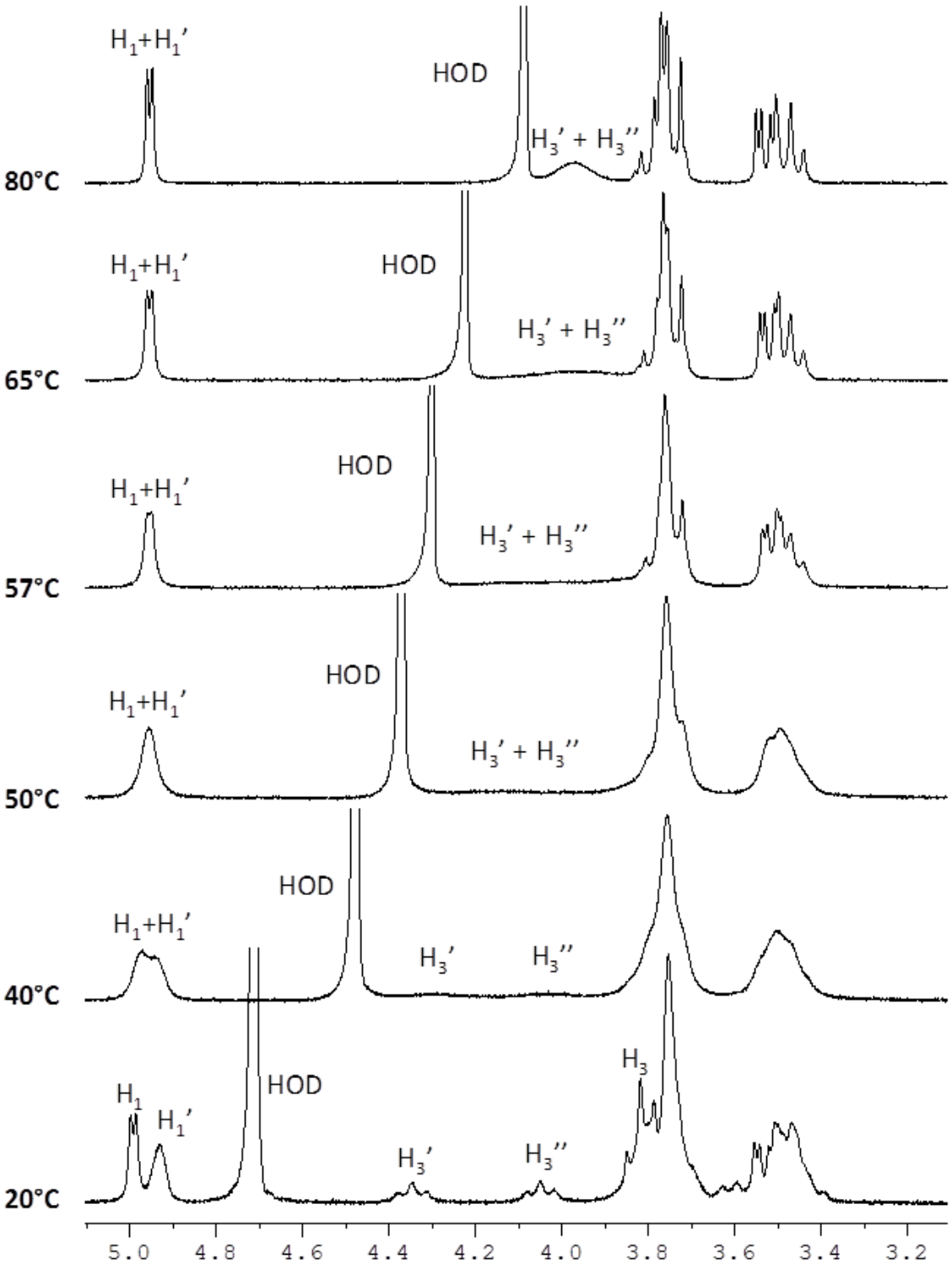

Figure S13. Variable temperature ^{1}H NMR spectra of γ-CD solution (3 mM) containing $[Ta_6Br_{12}(H_2O)_6]Br_2$ in the molar ratio $[Ta_6Br_{12}(H_2O)_6]^{2+}$/CD = 0.25, showing magnetization exchange between protons of free (H_n) and complexed (H_n') CDs, and protons of the two types of glucopyranose units (H_n' & H_n") present in the complexed CD.

5.8. COSY ^{1}H NMR

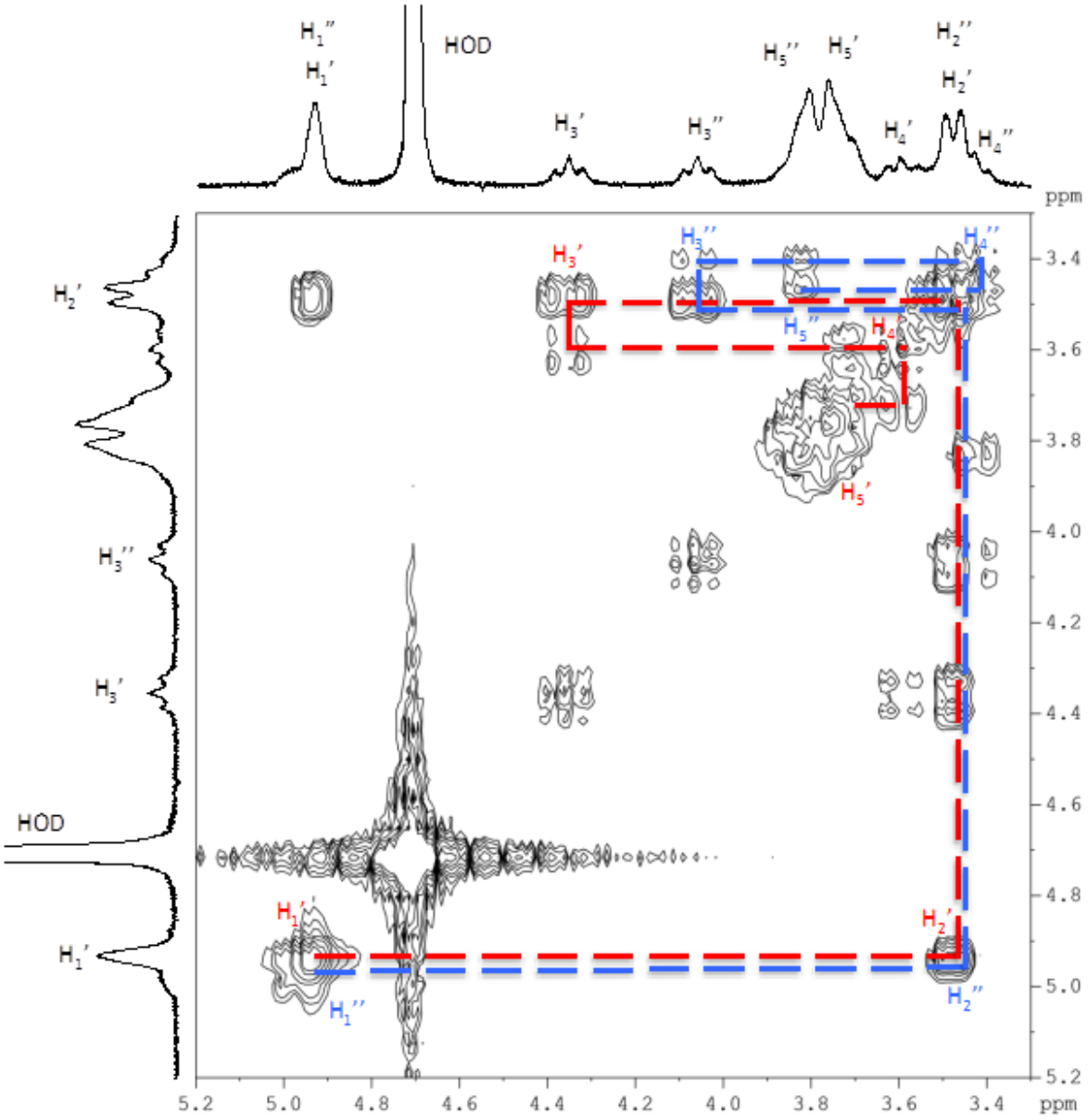

Figure S14. ^{1}H COSY NMR spectrum of γ-CD solution (3 mM) containing $[Ta_6Br_{12}(H_2O)_6]Br_2$ in the molar ratio $[Ta_6Br_{12}(H_2O)_6]^{2+}$/CD = 2.3, showing correlations between resonances of the two distinguished glucopyranose units (H_n' & H_n") present in the complexed CD.

6. ESI-Mass spectrum of the {Ta_6}@2CD complex in aqueous solution .

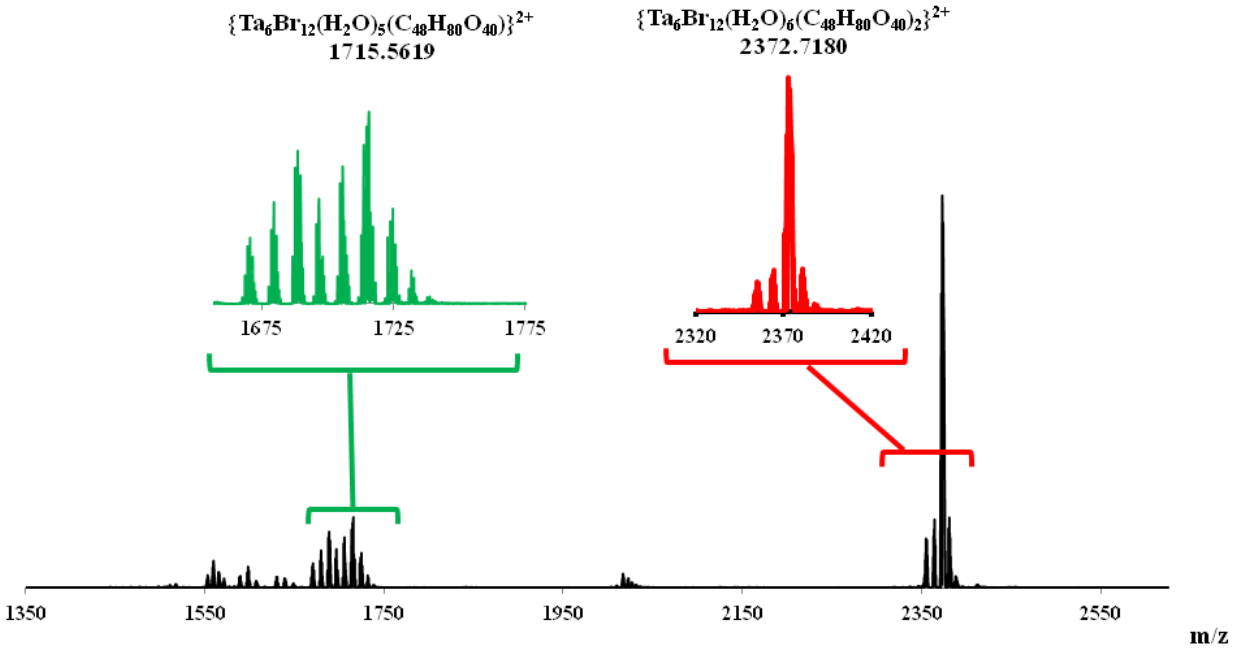

Figure S15. ESI-MS spectrum of the inclusion compound in aqueous solution{Ta_6}@2CD containing the m/z peak related to the 1:2 (red trace) and 1:1 (green trace) adducts. The side peaks separated from each other by m/z = 9 are unambiguously attributed to either hydrated or dehydrated complexes.

7. ITC measurements and analysis.

Formation constants and inclusion enthalpies were simultaneously determined for each γ-CD/$[P_2W_{18}O_{62}]^{6-}$, γ-CD/$[Ta_6Br_{12}(H_2O)_6]^{2+}$ and γ-CD/$[P_2W_{18}O_{62}]^{6-}$/$[Ta_6Br_{12}(H_2O)_6]^{2+}$ systems by the use of an isothermal calorimeter (ITC_{200}, MicroCal Inc., USA).

7.1. Experimental conditions

Degassed deionised water solutions were used in both cell (V_0 = 202.8 µL) and syringe (40 µL). After addition of an initial aliquot of 0.2 µL, 10 aliquots of 3.7 µL of the syringe solution were delivered over 7 s for each injection. This number of ten injections was chosen according to Tellinghuisen's recommendation (J. Tellinghuisen, J. Phys. Chem. B 2005, 109 (42), 20027-20035). The time interval between two consecutive injections was 90 s, which proved to be sufficient for a systematic and complete return to baseline (when no gelation phenomenon was observed in the cell). The agitation speed was set to 1000 rpm. The resulting heat flow was recorded as a function of time.

Experiments involving γ-CD/$[P_2W_{18}O_{62}]^{6-}$ and γ-CD/$[Ta_6Br_{12}(H_2O)_6]^{2+}$ binary systems :

Since mixtures of 1:1 and 1:2 complexes were expected, two distinct ITC titrations were realized at three temperatures (283, 298 and 313 K), in order to merge experimental information on both complexes. Titration 1 was implemented by using a cell filled with a guest solution and a syringe filled with a γ-CD solution. Titration 2 involved a cell filled with an equimolar solution of host and guest, and a syringe filled with a γ-CD solution. The following concentrations were used for the different systems :

Guest		**Cell**	**Syringe**
$[P_2W_{18}O_{62}]^{6-}$	Titration 1	$[P_2W_{18}O_{62}]^{6-}$ 0.125 mM	γ-CD 2.5 mM
	Titration 2	$[P_2W_{18}O_{62}]^{6-}$ 0.25 mM + γ-CD 0.25 mM	γ-CD 2.5 mM
$[Ta_6Br_{12}(H_2O)_6]^{2+}$	Titration 1	$[Ta_6Br_{12}(H_2O)_6]^{2+}$ 0.33 mM	γ-CD 3.33 mM
	Titration 2	$[Ta_6Br_{12}(H_2O)_6]^{2+}$ 0.67 mM + γCD 0.67 mM	γ-CD 3.33 mM

Experiments involving γ-CD/$[P_2W_{18}O_{62}]^{6-}$/$[Ta_6Br_{12}(H_2O)_6]^{2+}$ ternary system :

Titrations were realized at 298 K by injecting a 200 µM $[P_2W_{18}O_{62}]^{6-}$ solution on a solution containing $[Ta_6Br_{12}(H_2O)_6]^{2+}$ (90 µM) and γ-CD (respectively 22.5, 90 and 360 µM for titration 1, 2 and 3).

7.2. Thermograms treatment

The heat of dilution of each partner was eliminated from each titration by subtracting the raw signal obtained for the corresponding blank titrations (i.e. only one partner in cell or syringe, the other compartment being filled with water). The peak area following each addition was obtained by integration of the resulting signal and was expressed as the heat effect per injection.

7.2.1. Isotherms treatment for γ-CD/$[P_2W_{18}O_{62}]^{6-}$ and γ-CD/$[Ta_6Br_{12}(H_2O)_6]^{2+}$ binary systems

Binding constants and inclusion enthalpies were determined by nonlinear regression analysis of the binding isotherms, using a dedicated homemade program (E. Bertaut, D. Landy, Beilstein J. Org. Chem. 2014, 10, 2630-2641).

Briefly, considering host and guest concentrations in syringe and in cell (before and after each injection), concentrations of each inclusion compound may be calculated by solving the binding polynomial corresponding to a mixture of 1:1 and 1:2 complexes.

These concentrations may then be used to calculate the variation, in the cell, of the number of moles, Δn_i, of any Cyclodextrin$_m$-Guest complex (CD_m-G), for each injection, according to equation (1) :

$$\Delta n_i = \left[[CD_m\text{-}G]_i * V_o - [CD_m\text{-}G]_{i-1} * (V_o - v_i) + \frac{[CD_m\text{-}G]_i * v_i - [CD_m\text{-}G]_{i-1} * v_i}{2} \right] \quad (1)$$

With v_i being the injected volume of the i^{th} injection.

Finally, the heat consecutive to each injection may be calculated by means of relation (2) :

$$Q_i = \Delta n_i^{CD\text{-}G} * \Delta H^{CD\text{-}G} + \Delta n_i^{CD_2\text{-}G} * \left(\Delta H^{CD\text{-}G} + \Delta H^{CD_2\text{-}G} \right) \quad (2)$$

It has to be stressed that $\Delta H^{CD_2\text{-}G}$ correspond to the formation of the 1:2 complex starting from the 1:1 complex (and not from the free species).

Relation (2) corresponds to the regression function for the least square fitting of the binding isotherms. This fitting is realized by means of Newton-Raphson algorithm, which minimizes the residual sum of squared deviations between experimental and theoretical data, by varying the thermodynamic parameters.

In order to ensure that data treatment is not over-parameterized, a global analysis of the 6 distinct experiments (two titrations at three temperatures) was realized for each host-guest system. The

least square fitting was simultaneously applied to all isotherms with one set of thermodynamic parameters (i.e. with a unique formation constant K, inclusion enthalpy ΔH and heat capacity variation ΔCp, for each complex), by means of van't Hoff law. T_0 being an arbitrary reference temperature, ΔG(T), ΔH(T), ΔS(T) and ΔC_p are linked by equations (3) to (5) :

$$K(T) = K(T_0) * e^{\left\{\frac{\Delta H(T_0)}{R}\left(\frac{1}{T_0}-\frac{1}{T}\right)+\frac{\Delta C_p}{R}\left(\ln\left\{\frac{T}{T_0}\right\}+\frac{T_0}{T}-1\right)\right\}} \quad (3)$$

$$\Delta H(T) = \Delta H(T_0) + \Delta C_p * (T - T_0) \quad (4)$$

$$\Delta G(T) = \Delta H(T) - T * \Delta S(T) \quad (5)$$

Such a global analysis of 6 distinct experiments not only allow a better discrimination between the equilibriums models, but it also increases the accuracy on each thermodynamic parameters, even in the case of weak formation constants.

Finally, uncertainties on each thermodynamic parameters were determined by a priori variance–covariance matrix[2]. Calculations of accuracy have been undertaken considering all isotherms, after global analysis of each system.

7.2.2. Isotherms treatment for γ-CD/$[P_2W_{18}O_{62}]^{6-}$/$[Ta_6Br_{12}(H_2O)_6]^{2+}$ ternary system

Thermodynamic parameters was obtained with the same scheme than for binary systems, but for only one temperature, and with binding polynomials and heat as described below.

In order to shorten equations, γ-CD, $[P_2W_{18}O_{62}]^{6-}$ and $[Ta_6Br_{12}(H_2O)_6]^{2+}$ are respectively abbreviated by CD, POM and $\{Ta_6\}$.

7.2.2.1. Hypothesis 1 : absence of hetero-ternary complexes

Considering only a competition between the previously described 1:1 and 1:2 γ-CD complexes of POM and {Ta6}, the total concentration of each partner are described by equations (6) to (8) :

$$[CD]_T = [CD] + [CD\text{-}\{Ta_6\}] + 2*[CD_2\text{-}\{Ta_6\}] + [CD\text{-}POM] + 2*[CD_2\text{-}POM] \quad (6)$$

$$[\{Ta_6\}]_T = [\{Ta_6\}] + [CD\text{-}\{Ta_6\}] + [CD_2\text{-}\{Ta_6\}] \quad (7)$$

$$[POM]_T = [POM] + [CD\text{-}POM] + [CD_2\text{-}POM] \quad (8)$$

Each of these three equations may then be developed by using the formations constants linked to each complex :

$$[POM] = \frac{[POM]_T}{1+K_{CD-POM}*[CD]+K_{CD_2-POM}*K_{CD-POM}*[CD]^2} \quad (9)$$

$$[\{Ta_6\}] = \frac{[\{Ta_6\}]_T}{1+K_{CD-\{Ta_6\}}*[CD]+K_{CD_2-\{Ta_6\}}*K_{CD-\{Ta_6\}}*[CD]^2} \quad (10)$$

$$[CD]_T - [CD] - K_{CD-\{Ta_6\}} * [CD] * [\{Ta_6\}] - 2 * K_{CD_2-\{Ta_6\}} * K_{CD-\{Ta_6\}} * [CD]^2 * [\{Ta_6\}] - K_{CD-POM} * [CD] * [POM] - 2 * K_{CD_2-POM} * K_{CD-POM} * [CD]^2 * [POM] = 0 \quad (11)$$

Equation (11) was solved numerically by the use of Newton's method, considering [CD] as the only variable (which enables the calculation of [POM] and $[\{Ta_6\}]$ by the use of equation (9) and (10), respectively). Once the correct value of [CD] is known, the concentration of all species can be calculated directly.

Finally, the heat consecutive to each injection may be calculated by means of relation (12) :

$$Q_i = \Delta n_i^{CD-POM} * \Delta H^{CD-POM} + \Delta n_i^{CD_2-POM} * (\Delta H^{CD-POM} + \Delta H^{CD_2-POM}) + \Delta n_i^{CD-\{Ta_6\}} * \Delta H^{CD-\{Ta_6\}} + \Delta n_i^{CD_2-\{Ta_6\}} * (\Delta H^{CD-\{Ta_6\}} + \Delta H^{CD_2-\{Ta_6\}}) \quad (12)$$

7.2.2.2. *Hypothesis 2 : presence of hetero-ternary complexes*

Considering that one POM molecule may possess three independent bindings sites for CD-$\{Ta_6\}$ and/or CD_2-$\{Ta_6\}$complexes, and also considering negligible concentrations for CD-POM and CD_2-POM complexes, the total concentration of each partner are described by equations (13) to (15):

$$[POM]_T = [POM] + \left[POM\text{-}\left[CD\text{-}\{Ta_6\}\right]\right] + \left[POM\text{-}\left[CD_2\text{-}\{Ta_6\}\right]\right] \quad (13)$$

$$[\{Ta_6\}]_T = [\{Ta_6\}] + \left[CD\text{-}\{Ta_6\}\right] + \left[CD_2\text{-}\{Ta_6\}\right] + \left[POM\text{-}\left[CD\text{-}\{Ta_6\}\right]\right] + \left[POM\text{-}\left[CD_2\text{-}\{Ta_6\}\right]\right] \quad (14)$$

$$[CD]_T = [CD] + \left[CD\text{-}\{Ta_6\}\right] + 2*\left[CD_2\text{-}\{Ta_6\}\right] + \left[POM\text{-}\left[CD\text{-}\{Ta_6\}\right]\right] + 2*\left[POM\text{-}\left[CD_2\text{-}\{Ta_6\}\right]\right] \quad (15)$$

In order to account for the effective number of POM binding sites, $[POM]_T$ correspond to the total concentration of POM multiplied by 3.

In addition, the heteroternary complexes are characterized by their formation constant :

$$K_{POM\text{-}[CD\text{-}\{Ta_6\}]} = \frac{[POM-[CD-\{Ta6\}]]}{[POM]*[CD-\{Ta6\}]]} \quad (16)$$

$$K_{POM\text{-}[CD_2\text{-}\{Ta_6\}]} = \frac{[POM-[CD_2-\{Ta6\}]]}{[POM]*[CD_2-\{Ta6\}]]} \quad (17)$$

Equations (13) to (15) may then be developed by using the formations constants linked to each complex :

$$[POM] = \frac{[POM]_T}{1+K_{POM\text{-}[CD\text{-}\{Ta_6\}]}*K_{CD\text{-}T} * [CD]*[\{Ta_6\}]+K_{POM\text{-}[CD_2\text{-}\{Ta_6\}]} * K_{CD_2\text{-}\{Ta_6\}}*K_{CD\text{-}\{Ta_6\}}*[CD]^2*[\{Ta_6\}]} \quad (18)$$

$$[\{Ta_6\}]_T - [\{Ta_6\}] - K_{CD-\{Ta_6\}} * [CD] * [\{Ta_6\}] - K_{CD_2-\{Ta_6\}} * K_{CD-\{Ta_6\}} * [CD]^2 * [\{Ta_6\}] - K_{POM-[CD-\{Ta_6\}]} * K_{CD-\{Ta_6\}} * [CD] * [\{Ta_6\}] * [POM] - K_{POM-[CD-\{Ta_6\}]} * K_{CD_2-\{Ta_6\}} * K_{CD-\{Ta_6\}} * [CD]^2 * [\{Ta_6\}] * [POM] = 0 \quad (19)$$

$$[CD]_T - [CD] - K_{CD-\{Ta_6\}} * [CD] * [\{Ta_6\}] - 2 * K_{CD_2-\{Ta_6\}} * K_{CD-\{Ta_6\}} * [CD]^2 * [\{Ta_6\}] - K_{POM-[CD-\{Ta_6\}]} * K_{CD-\{Ta_6\}} * [CD] * [\{Ta_6\}] * [POM] - 2 * K_{POM-[CD-\{Ta_6\}]} * K_{CD_2-\{Ta_6\}} * K_{CD-\{Ta_6\}} * [CD]^2 * [\{Ta_6\}] = 0 \quad (20)$$

The system formed by equations (19) and (20) is solved numerically by the use of Newton's method, considering [CD] and [$\{Ta_6\}$] as variables (which enable the calculation of [POM] by the use of equation (18)). Once the correct values of [CD] and [$\{Ta_6\}$] are known, the concentration of all species can be calculated directly.

Finally, the heat consecutive to each injection may be calculated by means of relation (21) :

$$Q_i = \Delta n_i^{CD-\{Ta_6\}} * \Delta H^{CD-\{Ta_6\}} + \Delta n_i^{CD_2-\{Ta_6\}} * \left(\Delta H^{CD-\{Ta_6\}} + \Delta H^{CD_2-\{Ta_6\}}\right) + \Delta n_i^{POM-[CD-\{Ta_6\}]} * \left(\Delta H^{CD-\{Ta_6\}} + \Delta H^{POM-[CD-\{Ta_6\}]}\right) + \Delta n_i^{POM-[CD_2-\{Ta_6\}]} * \left(\Delta H^{CD-\{Ta_6\}} + \Delta H^{CD_2-\{Ta_6\}} + \Delta H^{POM-[CD_2-\{Ta_6\}]}\right) \quad (21)$$

7.3. Results for γ-CD/$[P_2W_{18}O_{62}]^{6-}$ and γ-CD/$[Ta_6Br_{12}(H_2O)_6]^{2+}$ binary systems

ITC thermograms and isotherms for the γ-CD/$[P_2W_{18}O_{62}]^{6-}$ and the γ-CD/$[Ta_6Br_{12}(H_2O)_6]^{2+}$ binary systems are presented in Figure S15 and S16, respectively. Simulations of mixture of 1:1 and 1:2 complexes were required to obtain satisfying fits for both systems. Thermodynamic parameters are summarized in Table S2.

7.4. Results for γ-CD/$[P_2W_{18}O_{62}]^{6-}$/$[Ta_6Br_{12}(H_2O)_6]^{2+}$ ternary system

The thermograms obtained for titrations 1, 2 and 3 are presented in Figure S17.

Concerning titration 1, if one try to simulate the corresponding theoretical heats according to hypothesis 1 (i.e. competition between 1:1 and 1:2 γ-CD complexes of POM and {Ta_6}, without hetero-ternary complexes), negligible values are obtained (inferior to 0.1 µcal per injection). Indeed, the cluster complexes are far stronger than the POM complexes (cf Table S2), in such a way that no significant amount of CD-POM complex is formed. This means either that hetero-ternary complexes are present and that 1:1 and 1:2 complexes between γ-CD and POM may be neglected under these experimental conditions. As a result, we tried to simulate the binding isotherm according to hypothesis 2 (each POM molecule possess three independent bindings sites for CD-{Ta_6} and/or CD_2-{Ta_6} complexes). Under these experimental conditions, the concentration of CD_2-{Ta_6} was rather low when compared to CD-{Ta_6} ; thus, the formation constant and inclusion enthalpy of the POM-[CD_2-{Ta_6}] complex were approximated by the corresponding parameters of the POM-[CD-{Ta_6}] complex, during the fitting process. The corresponding fit is presented in Figure 11 (main text).

In the case of titrations 2 and 3, evident increases of viscosity inside the cell resulted in deformed peaks. As a consequence, no simulation of the binding isotherms has been investigated.

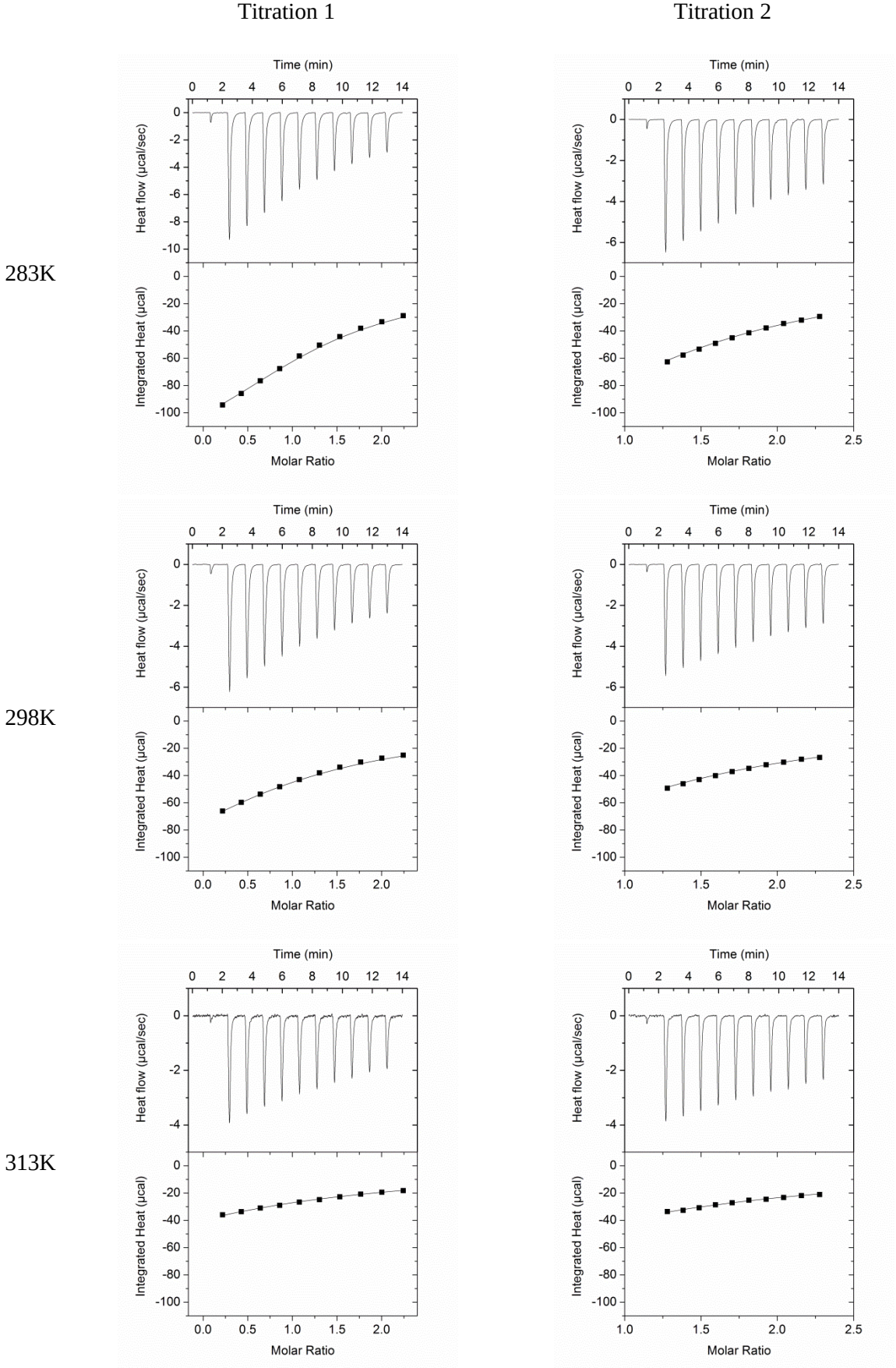

Figure S16. ITC thermograms (upper part) and isotherms (lower part) for the system γ-CD/$[P_2W_{18}O_{62}]^{6-}$. Dots and lines correspond to experimental and theoretical heats, respectively.

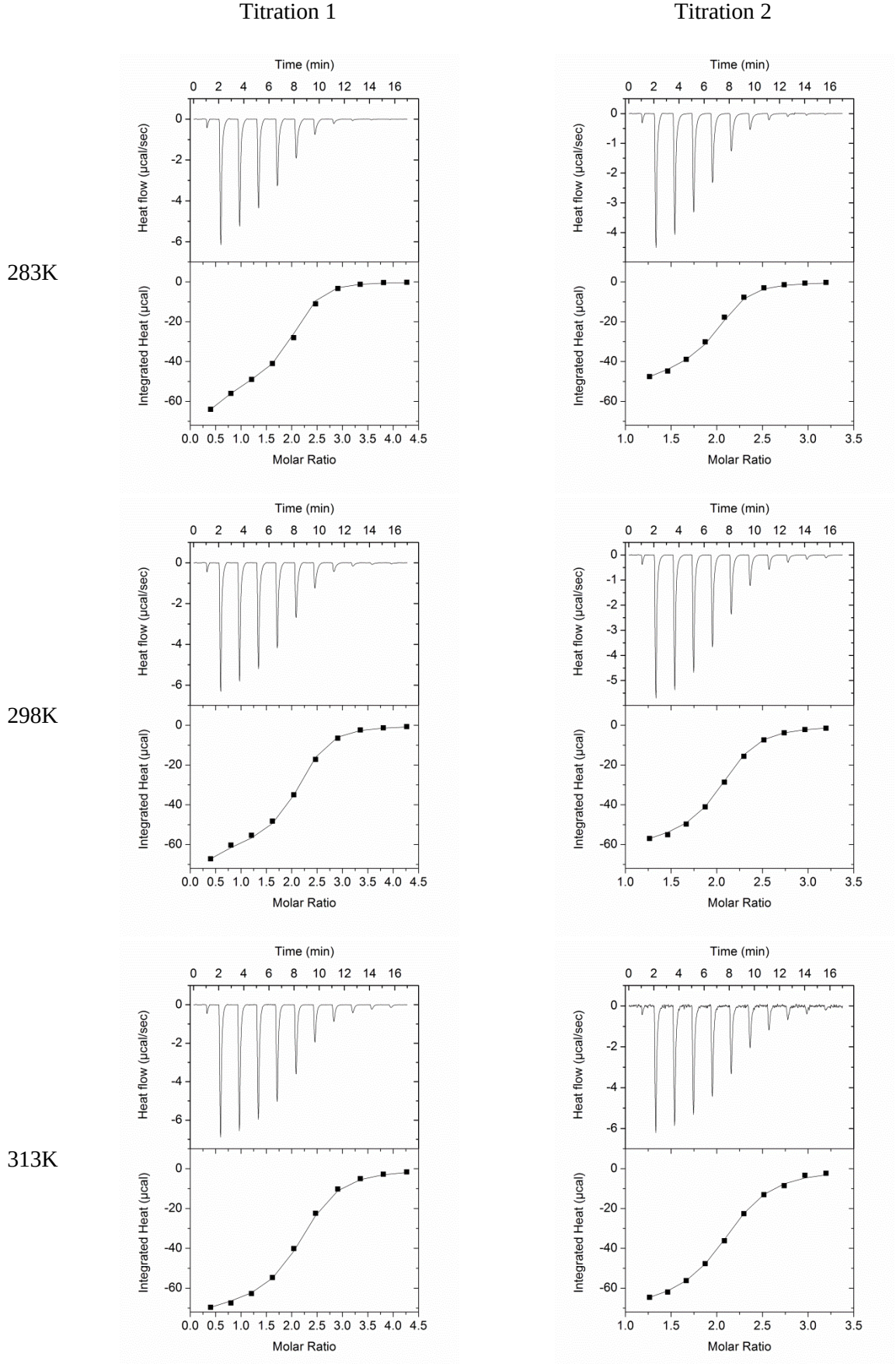

Figure S17. ITC thermograms (upper part) and isotherms (lower part) for the system γ-CD/$[Ta_6Br_{12}(H_2O)_6]^{2+}$. Dots and lines correspond to experimental and theoretical heats, respectively.

Table S2. Formation constant, enthalpy, entropy and free energy of inclusion, for the 1:1 and 1:2 complexes formed with γ-CD/$[P_2W_{18}O_{62}]^{6-}$ and γ-CD/$[Ta_6Br_{12}(H_2O)_6]^{2+}$ systems, obtained from ITC data, at 283, 298 and 313 K. Uncertainty rounded to the superior unit.

		T **(K)**	***K*** **(10^3 M^{-1})**	$\Delta_r H^*$ **(Kcal.mol^{-1})**	$T\Delta_r S^*$ **(Kcal.mol^{-1})**	$\Delta_r G^*$ **(Kcal.mol^{-1})**
POM	1:1	283	9,6 ± 0,5	-11,5 ± 0,2	-6,4 ± 0,3	-5,1 ± 0,1
	1:1	298	3,3 ± 0,2	-12,6 ± 0,5	-7,8 ± 0,6	-4,8 ± 0,1
	1:1	313	1,2 ± 0,1	-13,7 ± 0,8	-9,3 ± 0,8	-4,4 ± 0,1
	1:2	283	1,1 ± 0,2	-10,6 ± 0,8	-6,7 ± 0,9	-3,9 ± 0,1
	1:2	298	0,4 ± 0,1	-11,9 ± 1,6	-8,4 ± 1,7	-3,5 ± 0,2
	1:2	313	0,2 ± 0,1	-13,2 ± 6,9	-10,1 ± 7,0	-3,1 ± 0,2
{Ta6}	1:1	283	184,1 ± 4,8	-3,3 ± 0,2	3,6 ± 0,2	-6,8 ± 0,1
	1:1	298	127,2 ± 3,3	-5,1 ± 0,2	1,9 ± 0,2	-7,0 ± 0,1
	1:1	313	78,4 ± 2,1	-6,9 ± 0,2	0,1 ± 0,2	-7,0 ± 0,1
	1:2	283	315,7 ± 37,4	-7,9 ± 0,2	-0,8 ± 0,2	-7,1 ± 0,1
	1:2	298	153,3 ± 18,2	-8,2 ± 0,2	-1,2 ± 0,3	-7,1 ± 0,1
	1:2	313	77,6 ± 9,2	-8,6 ± 0,2	-1,6 ± 0,3	-7,0 ± 0,1

Titration 1

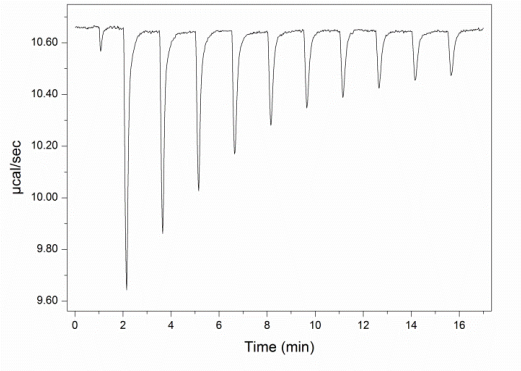

Titration 2

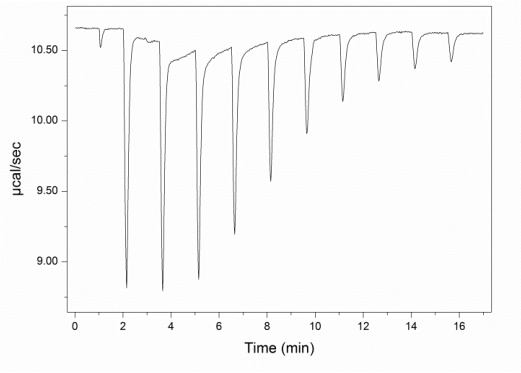

Titration 3

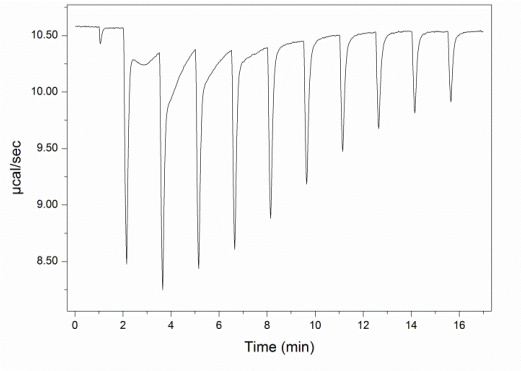

Figure S18. ITC thermograms obtained for γ-CD/$[P_2W_{18}O_{62}]^{6-}$/$[Ta_6Br_{12}(H_2O)_6]^{2+}$ ternary system. Injections, at 298 K, of 200 µM $[P_2W_{18}O_{62}]^{6-}$ on $[Ta_6Br_{12}(H_2O)_6]^{2+}$ (90 µM) and γ-CD (respectively 22.5, 90 and 360 µM for titration 1, 2 and 3).

8. UV-vis spectroscopy of the $\{Ta_6\}$ / γ-CD system

In the visible region, the electronic spectra of $[Ta_6Br_{12}(H_2O)_6]^{2+}$ cluster in aqueous solution is dominated by charge-transfer Ta→Ta transitions and Ta→Br (see Figure S18). The main UV-vis data are collected in Table S3. In the presence of various amount of γ-CD, the UV-vis spectrum of the of $[Ta_6Br_{12}(H_2O)_6]^{2+}$ cluster undergoes tiny changes mainly characterized by a "red" shift of the two band initially located at λ_{max} = 743 nm and λ_{max} = 648 nm.

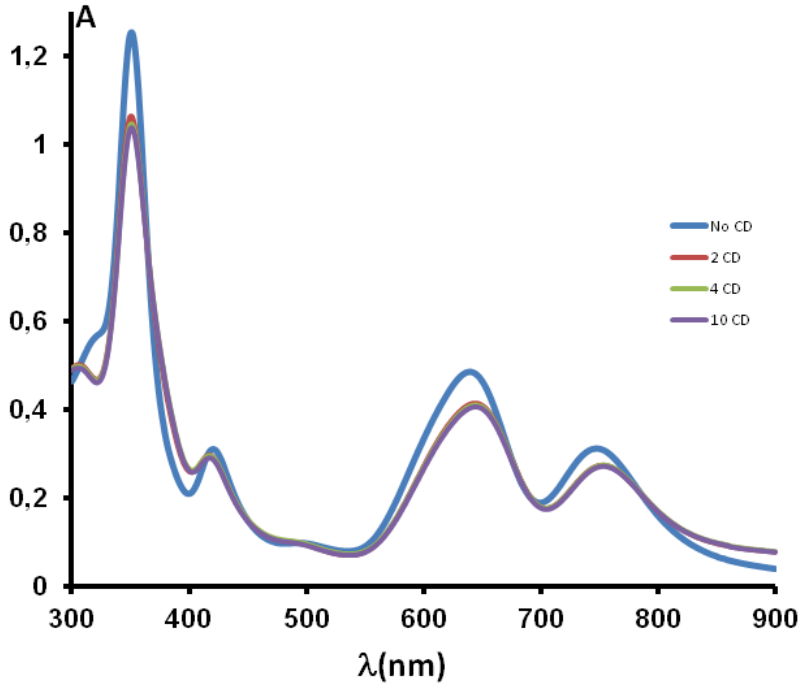

Figure S19. UV-vis spectra of $[Ta_6Br_{12}(H_2O)_6]^{2+}$ aqueous solution in presence solution in presence 0, 2, 4 and 10 γ-CD equivalents. For amount of γ-CD upper than 2 equivalents, the UV-vis features of the $\{Ta_6\}^{2+}$ cluster remain almost unchanged.

Table S3 : UV-vis data of the $[Ta_6Br_{12}(H_2O)_6]^{2+}$ cluster and the host-guest $\{[Ta_6Br_{12}(H_2O)_6]@2CD\}^{2+}$ assembly in aqueous solution with concentration ranging between 10^{-4} and $8\ 10^{-4}$ mol.L^{-1}.

Compound	**λ_{max} (nm) / ε (mol^{-1}Lcm^{-1})**
$[Ta_6Br_{12}(H_2O)_6]Br_2$	354 / 15 125; 420 / 3 875 ; 640 / 6 000 ; 745 / 3 875
$\{[Ta_6Br_{12}(H_2O)_6]@2CD\}Br_2•8H_2O$	354 / 13 250 ; 418 / 3 625 ; 648 / 5 125 ; 751 / 3 375